'Polysaccharides nanocomposites with Ca^{2+} and their multifunctional applications'

Prof. Farid Khan

Nanomaterials Discovery Lab. Department of Chemistry
Dr. H. S. Gour Central University
SAGAR- 470 003(M.P.)
E-mail: farid.fk@rediffmail.com, M-91-9425626334

- **Introduction**
- **Synthesis**
- **Characterization**
- **Applications**
  (a) Catalytic reduction of Cr(VI) to Cr(III)
  (b)Sensors for Cr(VI)
- **Thermodynamic Parameters**
  ΔG, ΔH, ΔS, ΔE, & TOF

Synthesis

1. Alg/CMC/Dex/Ca

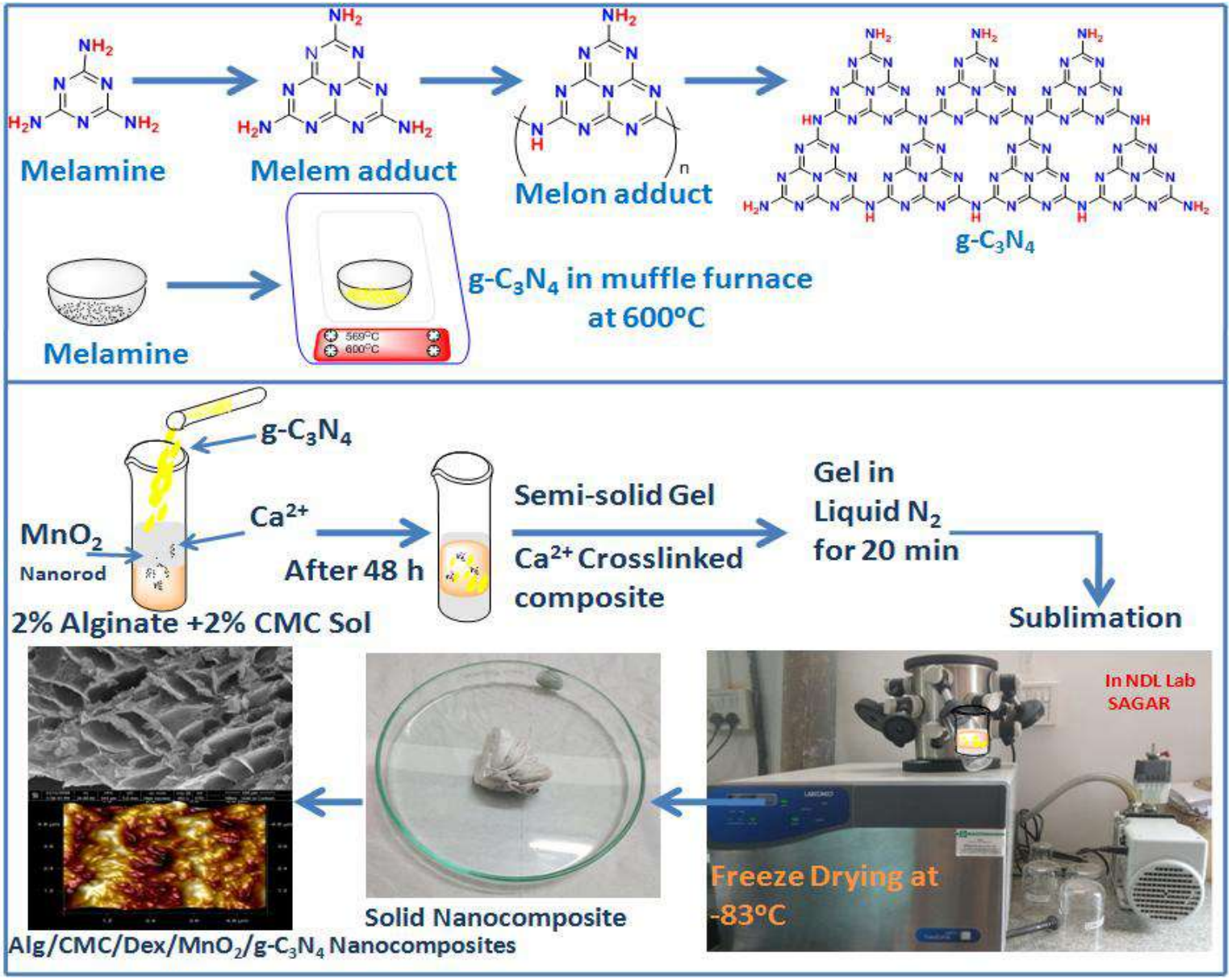
2. Alg/CMC/Dex/MnO_2/Ca

3. Alg/CMC/Dex/MnO_2/g-C_3N_4/Ca

Synthesis of g-C_3N_4

For the synthesis of g-C_3N_4 facile thermal polymerization method is used. Briefly, 5 g of melamine was put into an alumina crucible with a semi-enclosed lid in an Elite muffle furnace and heated to 600°C with a rate of 1°C/min for 6 h; the yellow product was collected after cooling.[31]

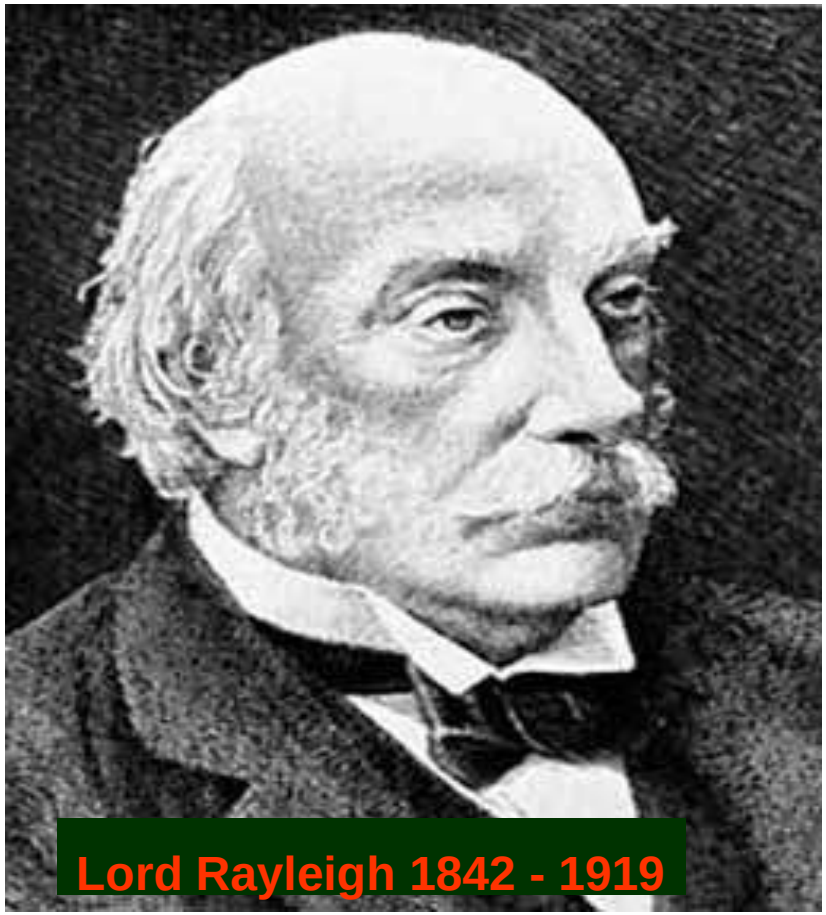
D. Ahirwar, M. Bano, I. Khan, S. S. Gond, MUD Sheikh, R. Mondal, & **Farid Khan, J. Solid State Chem., 2019, 273, 233-242.**



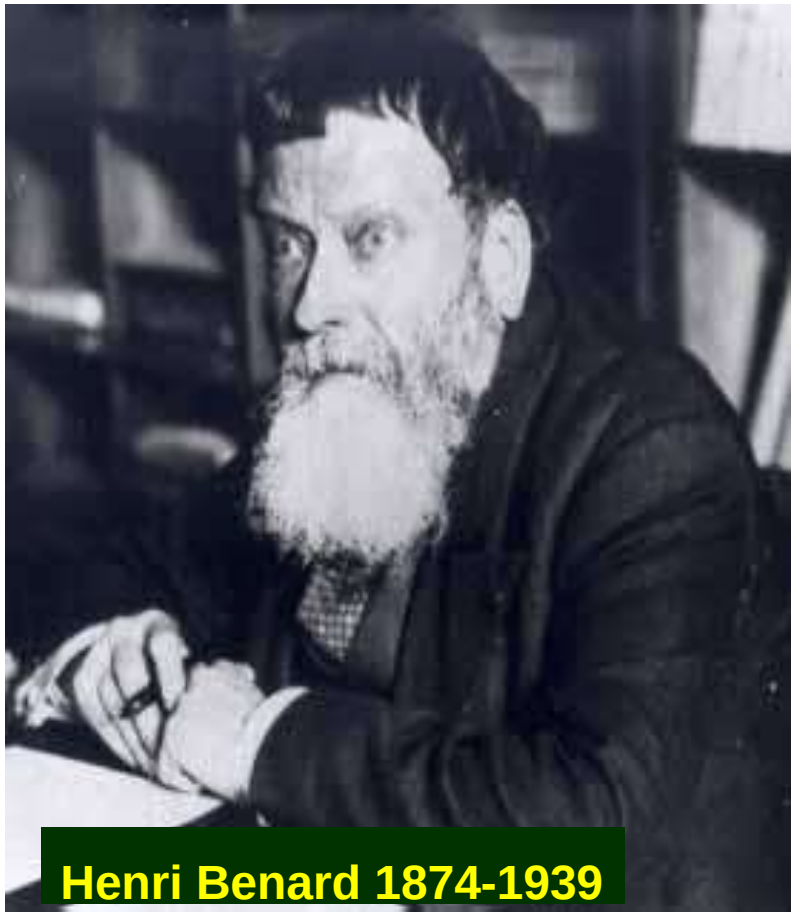
Scheme : Schematic set up of synthesizing of **Alg/CMC/Dex/MnO_2/g-C_3N_4/Ca composite**

M. Bano, I. Khan, D. Ahirwar and Farid Khan, React. And Funct. Polym., 2020, 150, 104545(1-15).

The Legacy of Henry Benard and Lord Rayleigh



Lord Rayleigh 1842 - 1919



Henri Benard 1874-1939

Rayleigh-Benard Convection

M. Thomas, G. A. Naikoo, M. U. Din Sheikh, M. Bano & Farid Khan, New J. Chem., 2015, 39, 9761-9771.

Rayleigh-Benard Heat Convection (Tube like pores with small pore network)

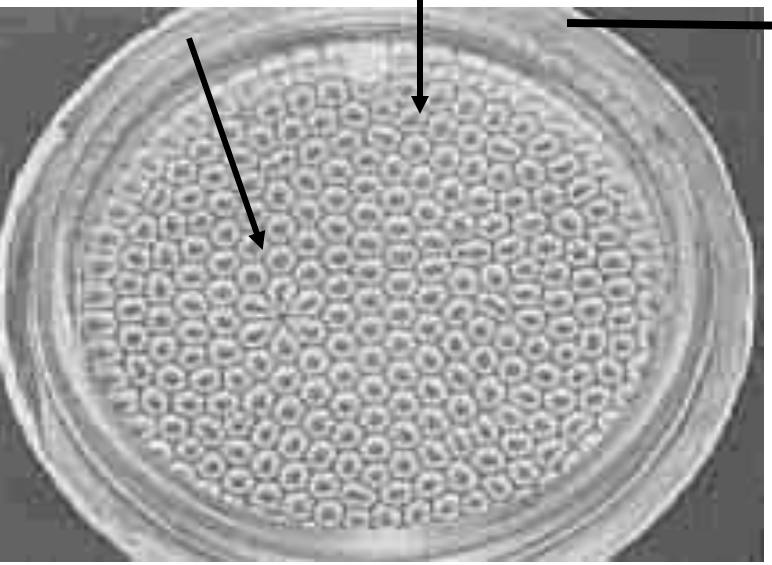


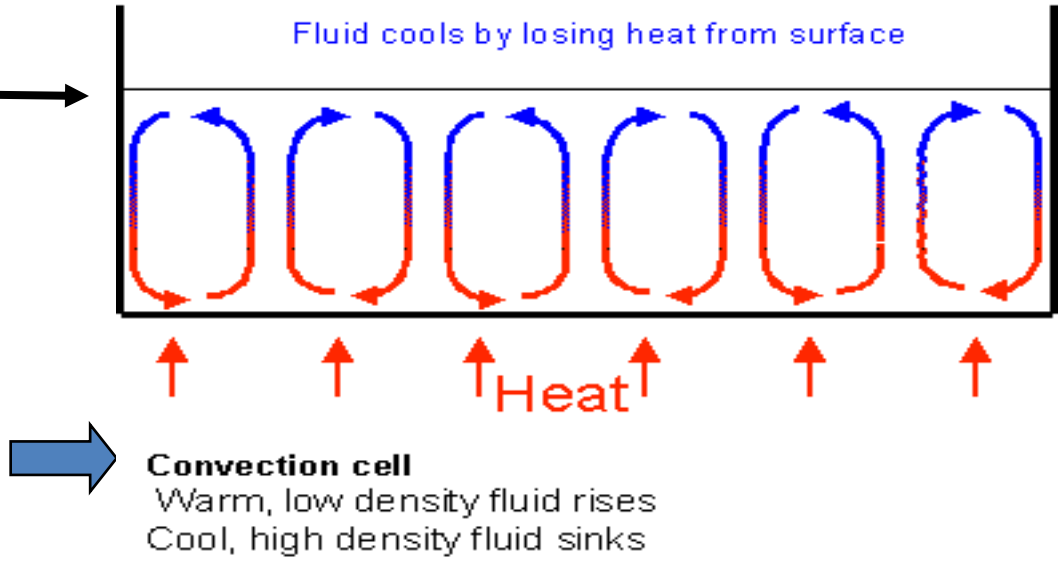
When a water pot is uniformly heated from below, the heated water of lower density flows upward and the cold water of higher density flows downward. Above a critical temperature difference between the bottom and the top of the pot, regular macroscopic convection cells (bodies/molecules move due to density difference due to T) can be detected.

These regular patterns are typical examples of ordered dissipative structures(self-organized structures, thermodynamically non equilibrium), but as soon as the driving force that keeps them far from equilibrium vanishes, ordering also ceases to exist and the structures disappear

Bénard cells

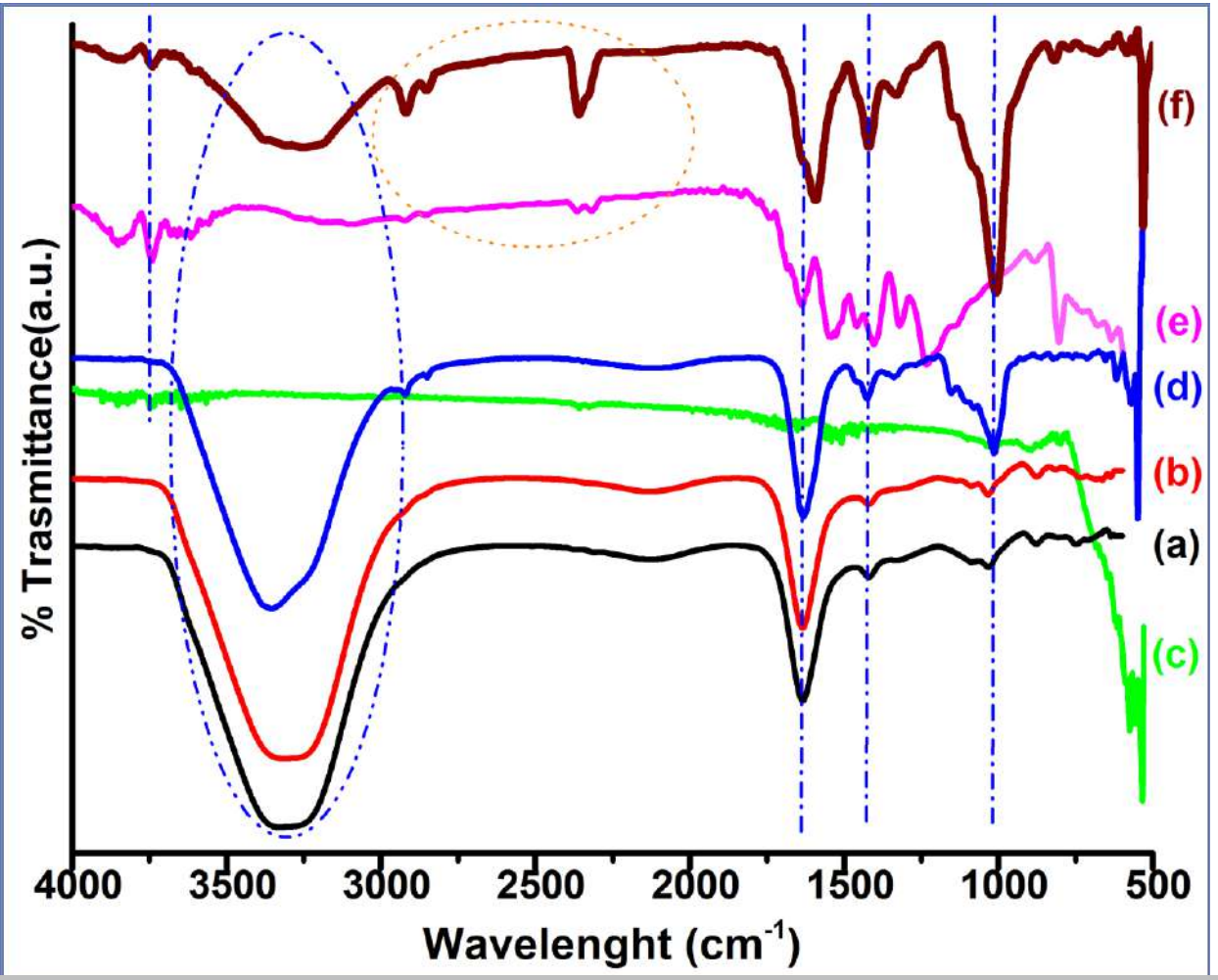
Top View



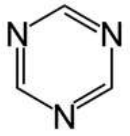


G. A. Naikoo, R. A. Daar and Farid Khan, J. Mater. Chem. A, 2014, 2, 11792-11798.

Characterization



Alg showed absorption peaks at 3400 cm^{-1}(ν_{-O-H}), 1627 cm^{-1}($\nu_{-C=O}$), 1411cm^{-1}(ν_{-COO} symmetric) and while CMC gave absorption peaks at 3442 cm^{-1} (ν_{-O-H}), 1627 cm^{-1} (ν_{-C-O}), and 1411 cm^{-1} (ν_{-COO} asymmetric vibration) respectively.[32] On crosslinking the Alg/CMC sol with Ca, there is a perturbation of frequency to lower side confirmed that Ca ions crosslinked Alg/CMC sol both. On addition of dextran to Alg/CMC sol, crosslinked with Ca, further perturbation of frequency is observed. Characteristic peaks of g-C_3N_4 were observed at 1200-1700 cm^{-1} as a result of stretching vibration modes of $C_{-N \text{ and } C=N}$ in heterocyclic ring. Peak located at 810 cm^{-1} (s-triazine ring) and 890 cm^{-1} (ν_{-N-H} bending).[33] In case of Alg/CMC/Dex/MnO_2/g-C_3N_4/Ca gel, there are peaks at 3250 cm^{-1}, 2348 cm^{-1} and all other peaks of g-C_3N_4 followed peak at 525 cm^{-1} due to MnO_2 which showed the presence of g-C_3N_4 and MnO2 nanorods in $_{Alg/CMC/Dex/MnO2}$/g-C_3N_4/Ca gel. Alg/CMC/Dex/MnO_2/g-C_3N_4/Ca gel also showed the required peaks as expected. Dextran also attributed its characteristic peaks in the corresponding monoliths.

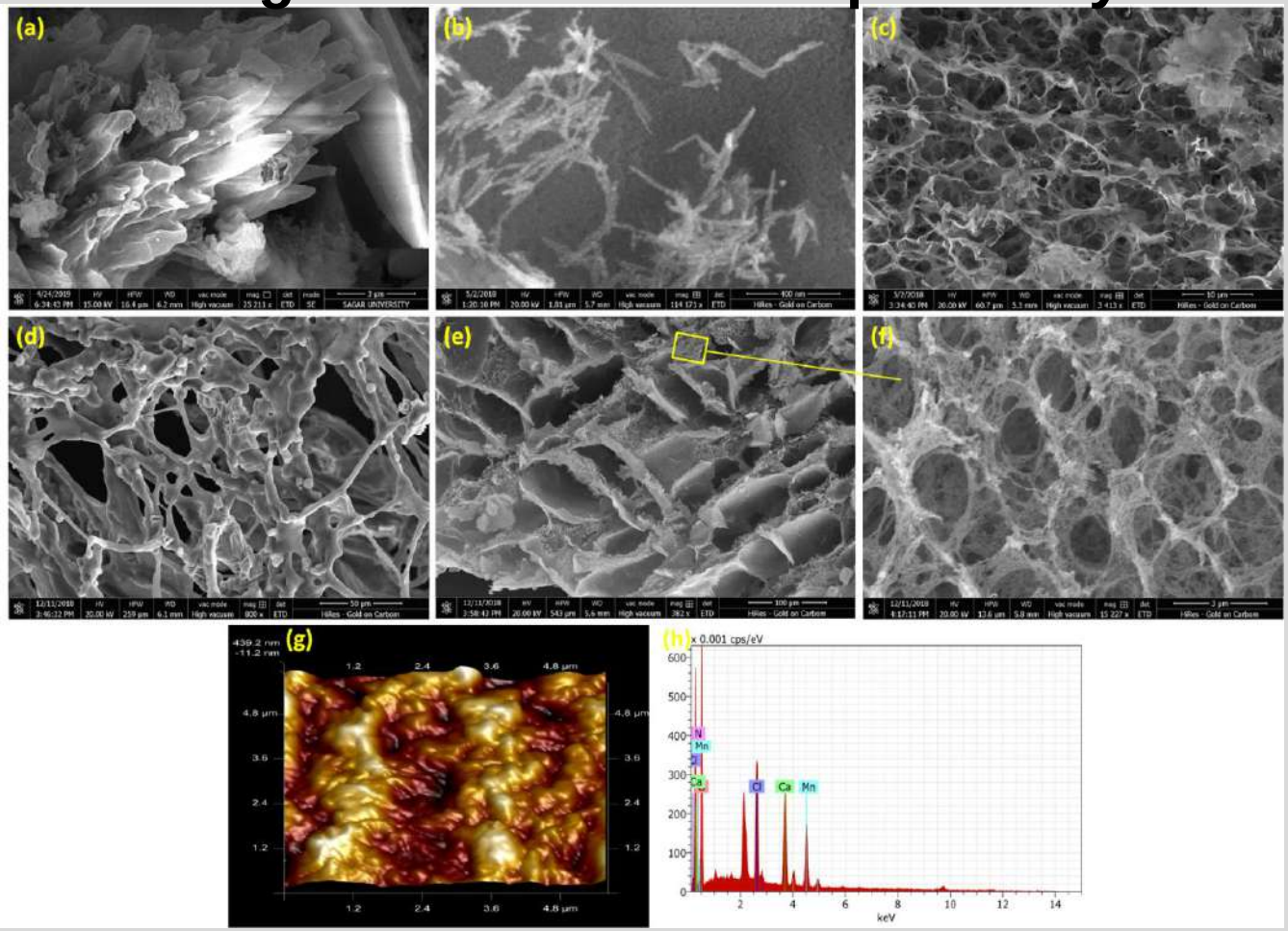


1,3,5 Triazine ring

Fig 1. Fourier Transform Infra Red Spectroscopic studies of (a) Alg/CMC/Ca, (b) Alg/CMC/Dex/Ca, (c) MnO_2 nanorod 200ºC (d) Alg/CMC/Dex/MnO_2/Ca, (e) bulk g-C_3N_4 (f) Alg/CMC/Dex/MnO_2/g-C_3N_4/Ca.

D. Ahirwar, M. Bano, I. Khan, S. S. Gond, MUD Sheikh, R. Mondal, & Farid Khan, J. Solid State Chem., 2019, 273, 233-242.

Scanning Electron Microscopic Study

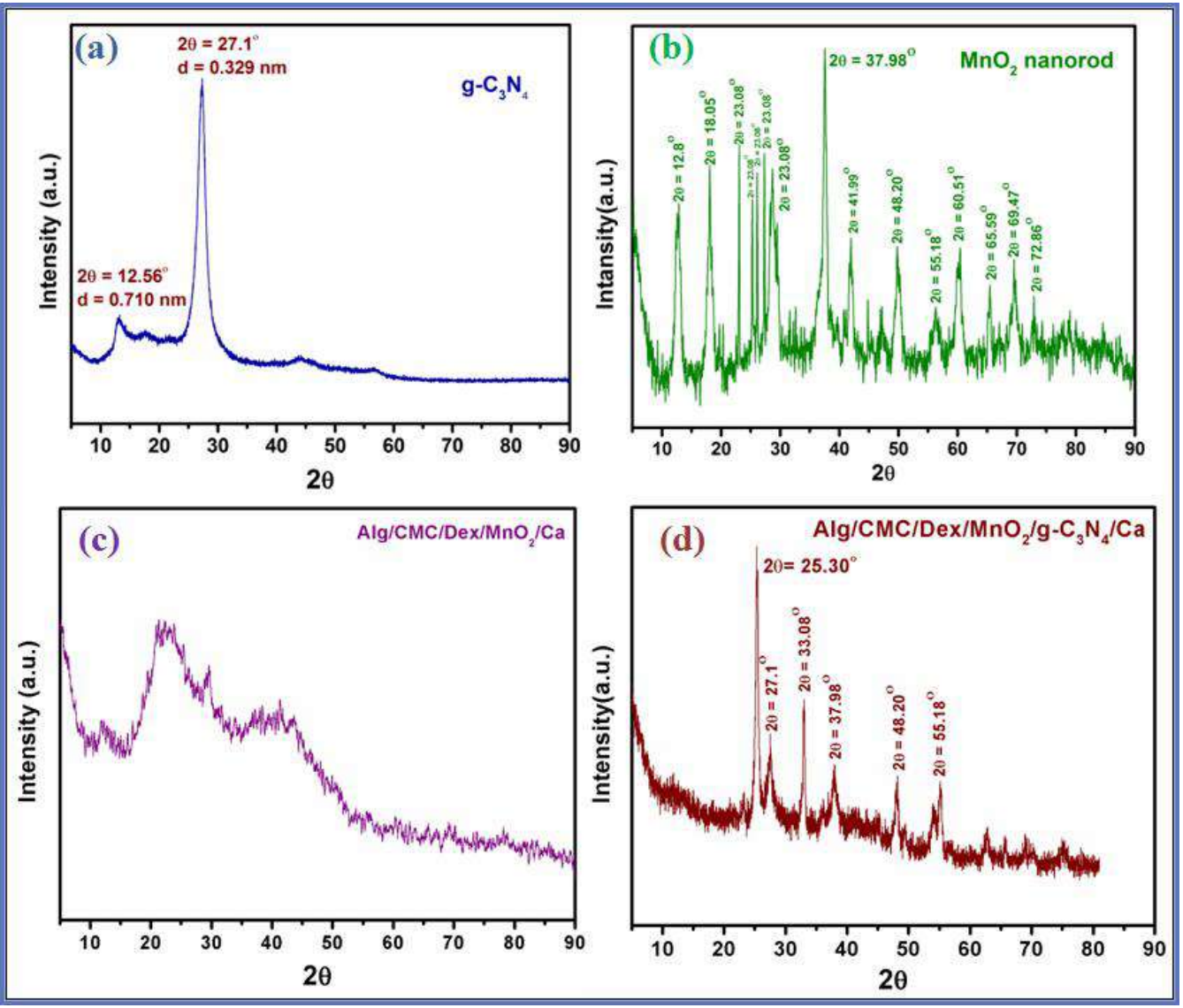


SEM images of Bulk-g-C_3N_4 is like fine grained shaped, were observed on the surface with charging on some of the petals of g-C_3N_4 structure (Fig.2 (a). Nanorods of MnO_2(200ºC) of length 100-500nm were clearly seen along with MnO_2 nanoparticles of size 10nm [Fig. 2(b)]. Alg/CMC/Dex/Ca composite (Fig. 2c) showed tube like pores with fragile morphology(scale bar 10µm). The Alg/CMC/Dex/MnO_2/Ca composite gel (Fig. 2d), exhibits a network of several ropes interconnected to each other in which MnO_2 nanoparticles of size 25 nm were clearly observed. Fig 2 e ,f are the images for Alg/CMC/Dex/MnO_2/g-C_3N_4/Ca composites showed the capillaries of diameters of sizes 50 - 100µm and on highlighting the specific area, small pores of sizes about 50nm to 1500nm were also formed(Fig.2f) with grained shaped structures showing the presence of g-C_3N_4 were also observed. AFM image (Fig 2g) of composite Alg/CMC/Dex/MnO_2/g-C_3N_4/Ca supported the morphology as observed in SEM(Fig. 2 e & f). EDAX analysis of composite Alg/CMC/Dex/MnO_2/g-C_3N_4/Ca showed the presence of MnO_2, and g-C_3N_4.

Fig. 2 Sem images of (a) Bulk g-C_3N_4, (b) MnO_2 nanorods (200ºC), (c) Alg/CMC/Dex/Ca, (d) Alg/CMC/Dex/MnO_2/Ca, (e) and (f) Alg/CMC/MnO_2/g-C_3N_4/Ca at 100µm, 3µm, (g) AFM images of Alg/CMC/Dex/MnO_2/g-C_3N_4/Ca and (h) EDAX of Alg/CMC/Dex/MnO_2/g-C_3N_4/Ca

D. Ahirwar, M. Bano, and Farid Khan, Journal of Solid State Chemistry, Volume 273, Year 2019, Pages 233-242, (IF – 2.8).

Powder X-Ray Diffraction Study

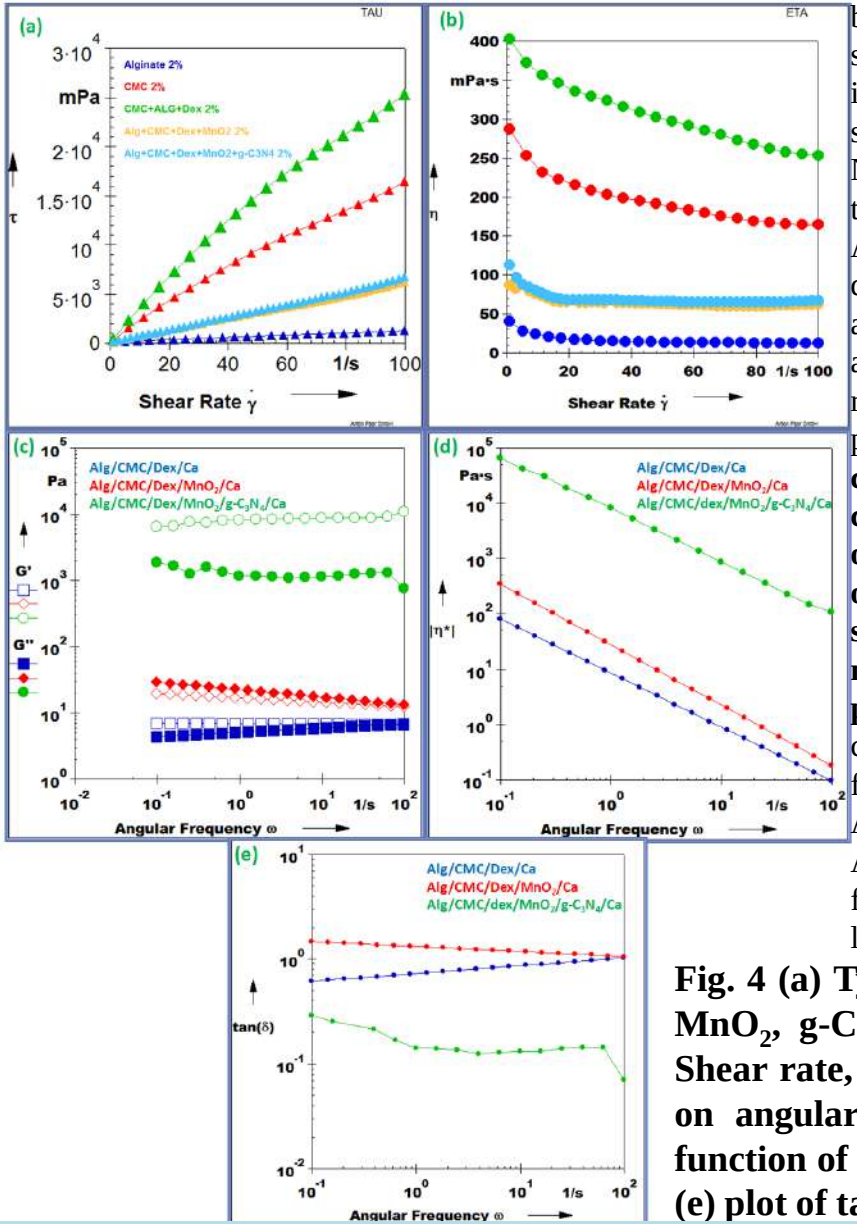


XRD pattern as depicted in Fig. 3, shows the characteristic peak of pure g-C_3N_4 at 27.1º Fig 3(a) the relatively weak peak at 12.5º (d=0.6676 nm) was assigned to (1 0 0) plane. Besides, the strong peak located at 27.1º corresponded to the stacking of conjugated aromatic (0 0 2) planes with the d-spacing of 0.1690 nm with Average crystalline size of monoliths 21.715 nm[34] The individual diffraction peaks of MnO_2 nanorod corresponds to the pure α-MnO_2 phase with a tetragonal crystal system at JCPDS No.44-0141.[35] **Alginate shows two characteristic peaks at 13.76° and 29.48° indicates amorphous structure** rather than crystalline. The CMC has a broad diffraction peak at 20.52°, indicating that CMC is partly crystalline.[36] **Composite Alg/CMC/Dex/MnO_2/Ca showed the amorphous behavior. O**n addition of g-C_3N_4 in situ to as synthesized Alg/CMC/Dex/MnO_2/Ca composite, it (Alg/CMC/Dex/MnO_2/g-C_3N_4/Ca) showed the **semi crystalline nature** with characteristic peaks at 25.30, 27.10, 33.08, 37.98, 48.20, 55.18, and 62.14º (Å) was assigned to (1 1 1), (-1 0 2), (-2 0 2), (2 3 0), (3 2 0), (1 1 3) and (0 0 4) respectively with Average crystalline size of monoliths 55.48 nm.

Fig.3.Powder X-ray diffraction pattern in length scale 5 to 90º (a) Pure g-C_3N_4,(b) Pure MnO_2 nanorod at 200°C, (c) Alg/CMC/Dex/MnO_2/Ca, & (d) Alg/CMC/Dex/MnO_2/g-C_3N_4/Ca.

M. Bano, I. Khan, & Farid Khan, Mater. Sci. & Engin. B, 2020(In Press)

Rheological Study

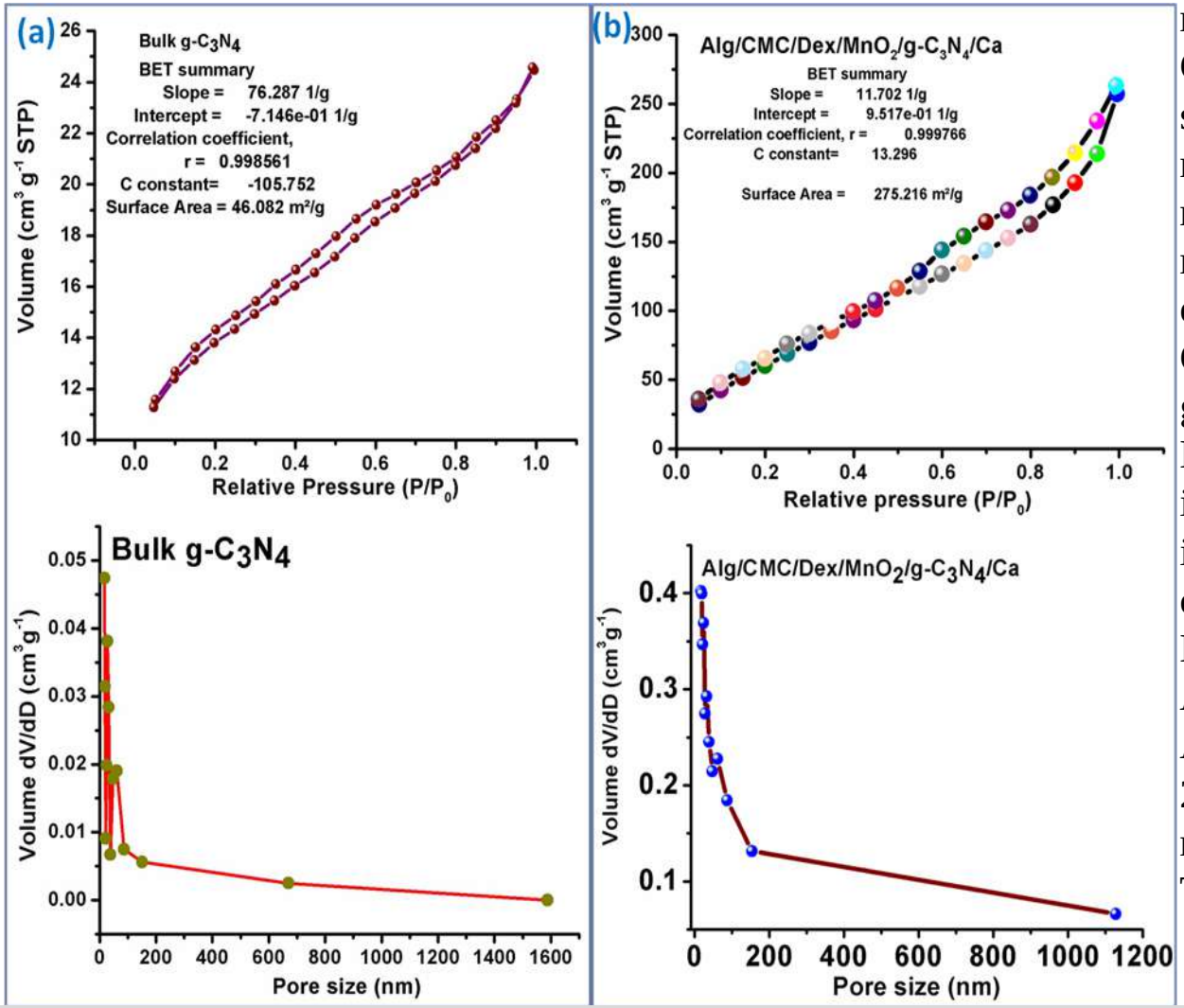


Rheological behaviours of sols of [Fig. 4(b)] Alginate 2%, CMC 2%, Alg/CMC/Dex/MnO_2, and Alg/CMC/Dex/MnO_2/g-C_3N_4 show Non-Newtonian behaviours intially however, they show Newtonian behaviour with increse of shear rate thereafter, Alg/CMC/Dex Sol shows non-Newtonian behaviour with increase of shear rate. Fig 4(a) shows the curves between shear stress (τ) and shear rate(Ẏ). All sols show Newtonian behavious. But sol Alg/CMC/Dex shows Newtonian behavious with increase of shear rate initially then it shows shear thining(non-Newtonian behaviour). In case of Alg/CMC/Dex/Ca and Alg/CMC/Dex/MnO_2/g-C_3N_4/Ca gels[Fig 4(c)], elastic behaviours are domination over viscous behaviour with increase of angular frequency sweep on account of showing gel like structures while Ag/CMC/Dex/MnO_2/Ca gel attributed viscous behaviour is greater than elastic behaviour over the entire region is owing to attenuation(reduction) of hydrogen bonding network which prevents the densification of gel network. **Fig. 4 (d), showed the behavior of complex viscosity (η*) against angular frequency(ω), for as synthesized composite gels, demonstrates a linear decrease in the viscosity with increase of frequency.[32] Structural transformations in the composite gels were observed due to breaking and reformation bonds. At higher frequency, structures do not get sufficient time for breaking and reformation of molecular bonds, and stable molecular alignment of extrication of long chain polysaccharides were observed which may diminish the complex viscosity**. In case of plot between damping factor (tan(δ) = G″/G′), against angular frequency(the values is lesser than 1 in case of Alg/CMC/Dex/Ca and Alg/CMC/Dex/MnO_2/g-C_3N_4/Ca composites except in case of Alg/CMC/Dex/MnO_2/Ca composite in the frequency range 0.1 to 100 rads^{-1}. The former gels showed elastic behaviors with stable crosslinked structures while later one showed the viscous behavior.

Fig. 4 (a) Typical strain-stress curves of Ca^{2+} ion crosslinked alginate,CMC, MnO_2, g-C_3N_4 composite gels; (b) Plots between viscosity coefficient and Shear rate, ((c) Dependence of storage modulus (G′) and loss modulus (G″) on angular frequency; (d) plot of complexdynamic viscosity (|η*|) as a function of angular frequency for the Alginate-CMC composites at 27ºC and (e) plot of tan (δ) as a function of angular frequency.

Khan, I. and Bano, M. and Khan, G.A. and Khan, F., Materials Science and Engineering B: Solid-State Materials for Advanced Technology, Volume 238-239, Year 2018, Pages 83-92

Surface Area Determnation



N_2 sorption and desorption studies of monoliths Alg/CMC/Dex/MnO_2/g-C_3N_4/Ca and g-C_3N_4 determined the surface area 275.216 and 46.082 m^2/g, respectively which might be the result of their nature of morphologies. Pore size distributions of both Alg/CMC/Dex/MnO_2/g-C_3N_4/Ca and g-C_3N_4 matrixes were given along with their BET graphs. Higher surface area benefits for increasing the active sites which increases the catalytic activity of the composite. The surface area of MnO_2(Nanorods, 200ºC), Alg/CMC/Dex/Ca, and Alg/CMC/Dex/MnO_2/Ca, were 25.89, 67.412 and 100.97 m^2g^{-1} respectively. Details are given in Table 1.

Fig 5(a). BET surface area and pore size distribution of bulk g-C_3N_4, (b) BET surface area and pore size distribution of Alg/CMC/Dex/MnO_2/g-C_3N_4/Ca.

Ahirwar, D. and Bano, M. and Khan, I. and Sheikh, M.U.-D. and Thomas, M. and Khan, F. ARTICLE Journal of Materials Science: Materials in Electronics, Volume 29, Year 2018, Pages 5768-5781 (IF – 2.01),

Table -1. Parameters for the reduction of Cr(VI) to Cr(III) at 25±0.5°C

Entry	Composites	d-spacing(Å)	Average Pore diameter (µm /nm)	Pore Volume (ccg^{-1})	Average crystalline size of monoliths (nm)	Surface area (m^2g^{-1})	% Conversion (min.)	Co-relation coefficient (R^2)
1	MnO_2	1.684	0.12567	0.002120	2.716405256	24.570	unchanged	0.901
2	g-C_3N_4	7.522	3.21293	0.003701	21.71580273	46.082	15	0.998
3	Alg/CMC/Dex/MnO_2/Ca	amorphous	3.81729	0.126100	amorphous	100.975	5	0.999
4	Alg/CMC/Dex/MnO_2/g-C_3N_4/Ca	11.265	5.78197	0.398000	55.48289145	275.216	1.20	0.999

Catalytic Activities of Silver composites

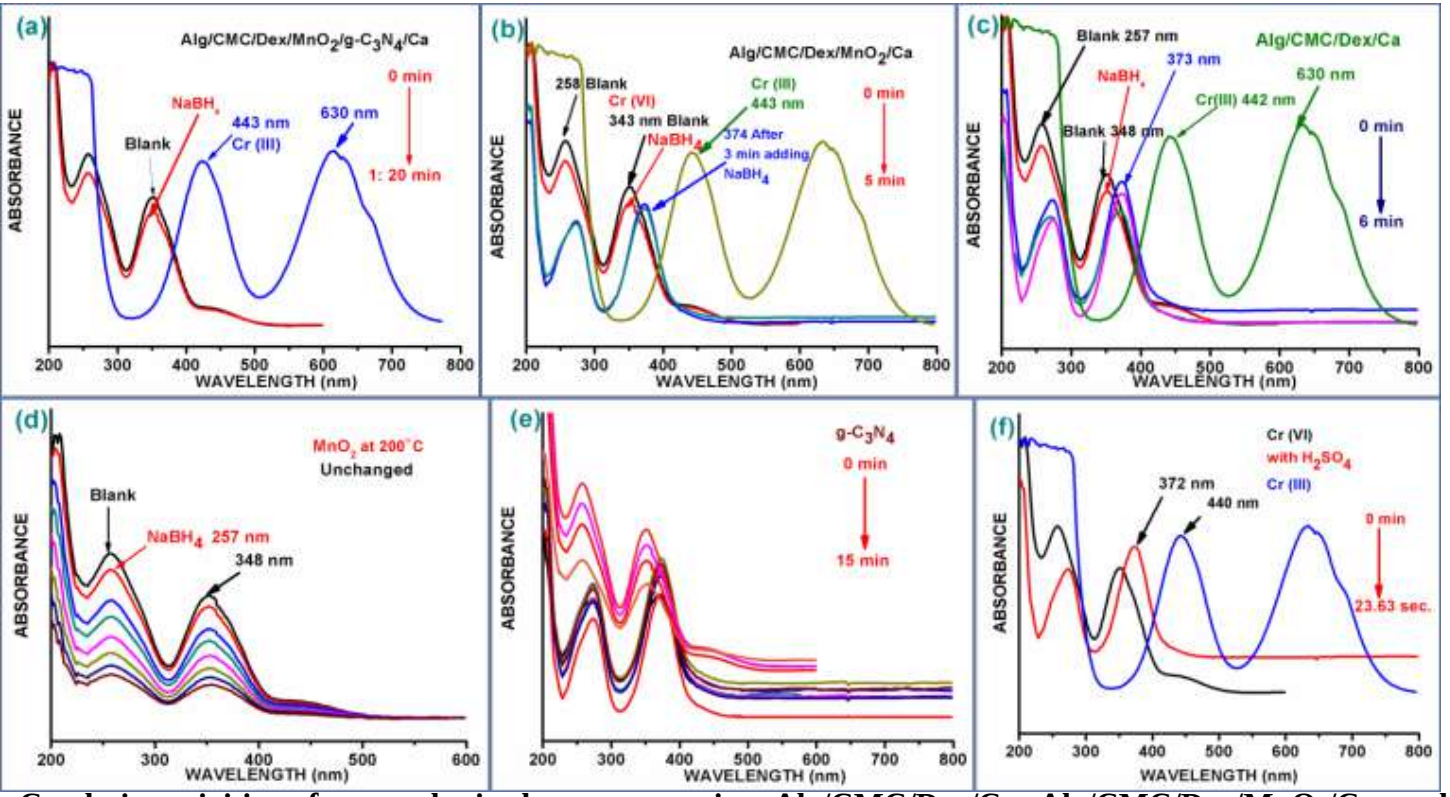


Fig. 6. UV–Vis spectra of reduction of Cr^{6+} to Cr^{3+} in presence of 0.1 M $NaBH_4$ by composites. (a) Alg/CMC/Dex./Mn O_2/g-C_3N_4/Ca, (b) Alg/CMC/Dex/MnO $_2$/Ca,(c) Alg/CMC/Dex/Ca, (d) MnO_2 nanorod, (e) g-C_3N_4, (f) Alg/CMC/Dex./Mn O_2/g-C_3N_4/Ca with H_2SO_4.

Catalytic activities of as synthesized nanocomposites Alg/CMC/Dex/Ca, Alg/CMC/Dex/MnO_2/Ca, and Alg/CMC/Dex/MnO_2/g-C_3N_4/Ca were studied in presence of 0.01M $NaBH_4$ by measuring the absorbance with wavelength for the reduction of chromium ions in Cr^{6+} to Cr^{3+} oxidation states in aqueous media (Fig. 6 a-f). 0.001M $K_2Cr_2O_7$ showed two intensive peaks at 257nm and 348 nm(Fig. 16 a) respectively are due to the transitions as per available.[45] (The band at 348 nm is assigned to A_{2g}-→$^4T_{1g}$(P) transition[46] while the band at 257nm is due to $^1A_1$ → $^1T_2$ transition[47]. When $NaBH_4$ is added to $K_2Cr_2O_7$ solution, no shift of bands is observed(Fig.6b) but as soon as catalyst Alg/CMC/Dex/MnO_2/g-C_3N_4/Ca(0.001g) was added to $K_2Cr_2O_7$ with $NaBH_4$ solution, two peaks at 442nm and 630nm were observed(Fig.6c) by d-d transition of Cr^{3+} ions in octahedral sites and are assigned to $^4A_{2g}$- → $^4T_{1g}$ & $^4A_{2g}$- → $^4T_{2g}$ transitions respectively[46]. Catalyst Alg/CMC/Dex/Ca, Alg/CMC/Dex/MnO_2/Ca reduced $K_2Cr_2O_7$(Yellow color) within 1.20 min and a greenish colour of Cr^{3+} ions was discernible (Fig.6).

Time taken by the composites Alg/CMC/Dex/MnO_2/Ca, Alg/CMC/Dex/Ca, and g-C_3N_4 matrix were 5, 6 and 15 min. while $NaBH_4$ alone does not show any catalytic activity to reduce Cr^{6+} to Cr^{3+} ions. When the reduction of Cr(VI) to Cr(III) is taken place in presence of 0.01M H_2SO_4, the composite catalyst Alg/CMC/Dex/MnO_2/g-C_3N_4/Ca took 23.63s. The mechanisms of the processes are given as

Thomas, M. and Sheikh, M.U.D. and Ahirwar, D. and Bano, M. and Khan, F., ournal of Colloid and Interface Science, Volume 505, Year 2017, Pages 115-129, Impact Factor – 7.30.

In presence of water

$$2Cr_2O_7^{--} + 4BH_4^- + 13H_2O \rightarrow 4Cr(OH)_3 + B_4O_7^{--} + 8OH^- + 11H_2$$ ---------- 1

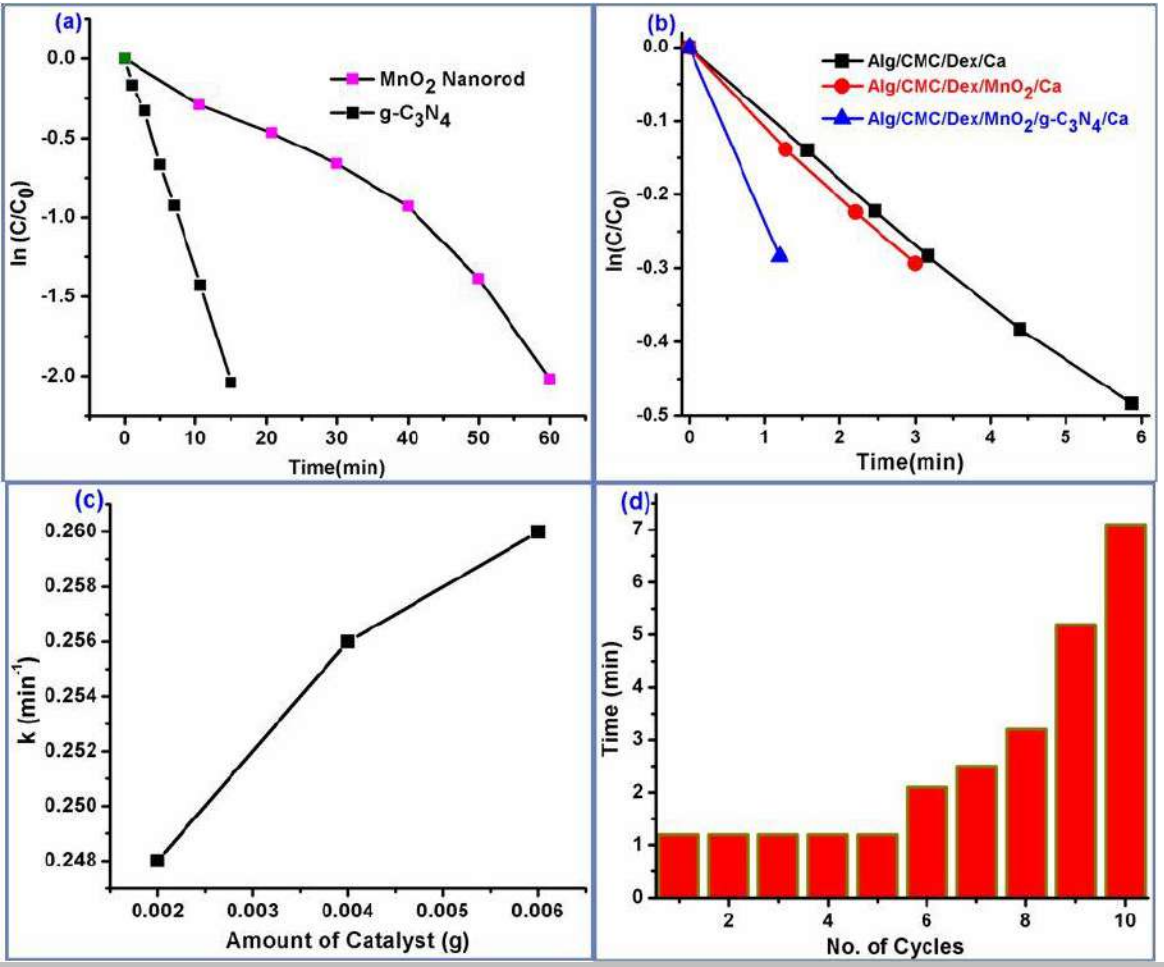
$$BH_4^- + 4H_2O \rightarrow B(OH)_4^- + 4H_2$$ ---------- 2

H_2 thus produced by $NaBH_4$ adsorbed at the surface of the catalyst reduces Cr(VI) to Cr(III). The pH of the potassium dichromate solution in water was 3.5. When $NaBH_4$ (0.01M) was added, the pH was 8.685. As soon as Catalyst Alg/CMC/Dex/MnO_2/g-C_3N_4/Ca was added to it, the pH was 2.40. Now the colour of the reactor solution is changing from **yellow to green** and on completion of the reduction of Cr(VI) to Cr(III), the pH recorded was 9.90. On addition of H_2SO_4 (1ml H_2SO_4, 0. 1M), in $K_2Cr_2O_7$ soln., the pH was 2.75. When $NaBH_4$ was added (the reaction mixture, the pH 7.234 and then Alg/CMC/Dex/MnO_2/g-C_3N_4/Ca was added, the pH was 8.591, and the time recorded was **23.63s f**or complete reduction of Cr(VI) to Cr(III). It is clear that the rate of reduction of Cr (VI) increased significantly in presence of acid.

$$2Cr_2O_7^{--} + 3BH_4^- + 19H^+ \rightarrow 4Cr^{3+} + 3H_3BO_3 + 6H_2 + 5H_2O$$ ---------- 3

Thomas, M. and Natarajan, T.S. and Sheikh, M.U.D. and Bano, M. and Khan, F. ARTICLE Journal of Photochemistry and Photobiology A: Chemistry, Volume 346, Year 2017, Pages 113-125,DOI:10.1016/j.jphotochem.2017.05.037 (IF – 3.0)

Chemical Dynamics



In case of composites Alg/CMC/Dex/Ca, Alg/CMC/Dex/MnO_2/g-C_3N_4/Ca, and Alg/CMC/Dex/MnO_2/Ca, the reaction kinetics **is pseudo first order** while g-C_3N_4, & MnO_2, matrix showed **zero order kinetics**. In presence of H_2SO_4, the composite Alg/CMC/Dex/MnO_2/gC_3N_4/Ca), showed **pseudo first order(Plot was not given).** The plots between the rate constant values were determined by d[C]/dt = k & $\ln(C/C_0)$ = kt respectively and given in Table 3. The plots between $\ln C/C_0$ Vs time were given in Fig. (a & b)

0.0002 to 0.001g

Fig. Kinetic study of Ca composites (a) Plots between $\ln C/C_0$ Vs Time for MnO_2(nanorods, 200°C) and g-C_3N_4 matrix (b) Plot between $\ln C/C_0$ Vs Time for Alg/CMC/Dex/Ca, Alg/CMC/Dex/MnO_2/Ca and Alg/CMC/Dex/MnO_2/g-C_3N_4/Ca composites (c) Plot between rate constant (k) Vs amount of catalyst for Alg/CMC/Dex/MnO_2/g-C_3N_4/Ca and (d) Recyclability of Alg/CMC/Dex/MnO_2/g-C_3N_4/Ca composite.

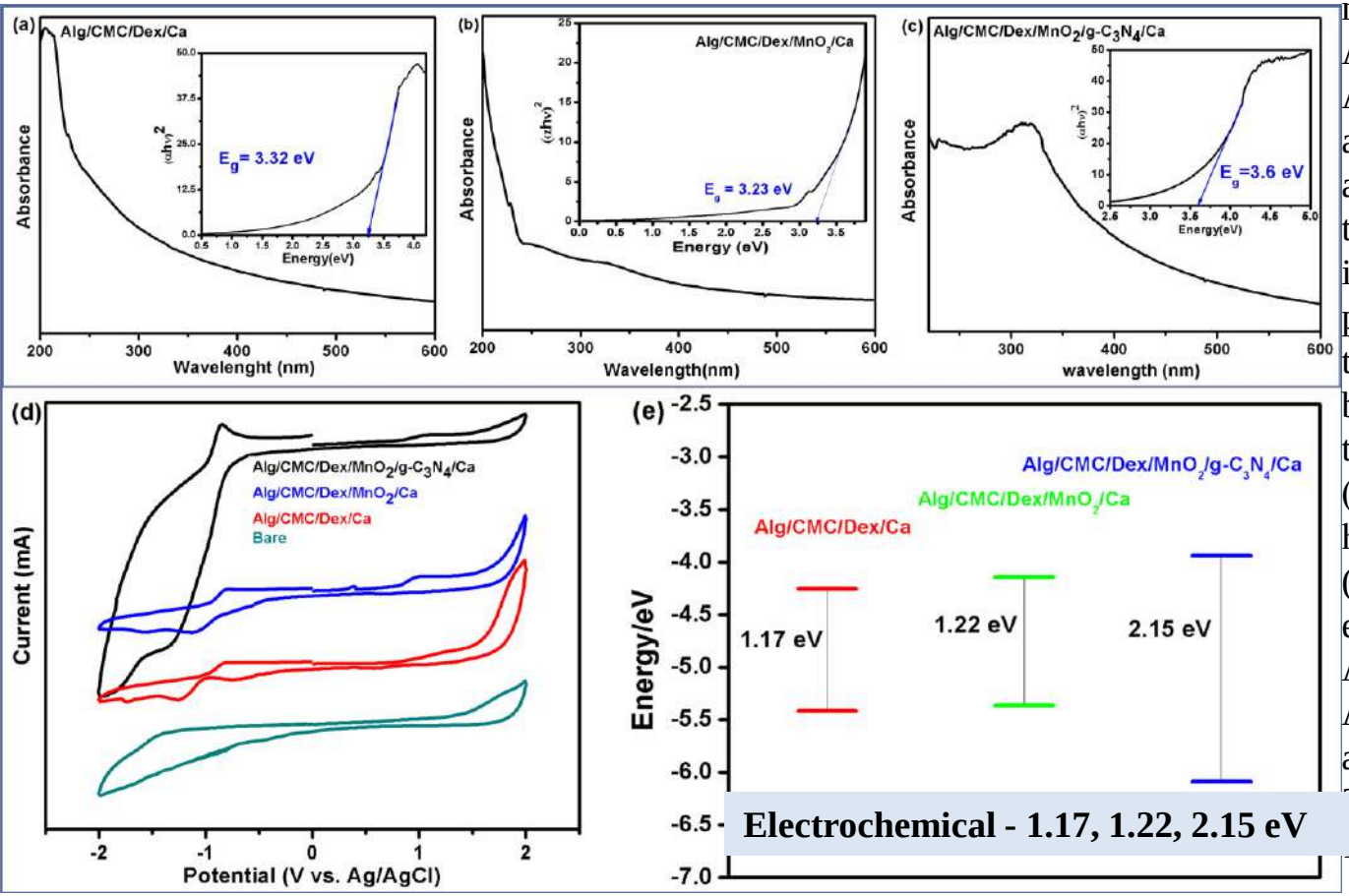
Bano, M. and Ahirwar, D. and Thomas, M. and Sheikh, M.U.D. and Khan, F.
ARTICLE Journal of Solid State Chemistry, Volume 248, Year 2017, Pages 40-50, IF – 3.5.

Kinetics of the reduction of Cr(VI) to Cr(III) is studied also by varying the amount of catalyst Alg/CMC/Dex/MnO_2/g-C_3N_4/Ca from 0.0002 to 0.001g at constant concentration of Cr(VI) at 0.1M $NaBH_4$ in aqueous solution and the rate constants were determined for pseudo first order reactions which increased from 0.248, 0.256 to 0.260 min^{-1} with consuming time 3, 2.4 and 1.20 min^{-1} respectively beyond concentration 0.008g the rate of the reaction became so fast that it cannot be measured under the present experimental conditions. Fig. d showed the stability & recyclability of the catalyst Alg/CMC/Dex/MnO_2/g-C_3N_4/Ca, it worked upto 10 cycles (first upto 5 cycle, it took the same time 1.20 min. then it took 2.20, 2.50, 3.0, 5.20& 7.10 min^{-1}). In each case, catalyst was separated by centrifugation (1200 rpm). The slight variation in time for the reduction of Cr(VI) to Cr(III) is due to small mass loss of the catalyst on account of handling and also the adsorption of Cr(III) on the surface of the catalyst which blocks its active sites.

Table -3

	Catalysts	Solvent/reducing agent	Convertion time	Order of the reaction	Ref
	PdNPs	Formic acid	5 min	first-order reaction	50
	$[\beta\text{-}As_8V_{14}O_{42}(H_2O)]^{4-}$	Formic acid	30 min	pseudo-first-order	51
	Pt-2 mol% $BiOC_{l0.8}Br_{0.2}$/alumina film			pseudo-first-order	52
	PdQDs	Acetic acid	5 min	Second order	53
	Pd-TMV	excess NaOH	30 min.	pseudo-first order	54
	PdCu nanoboxes	-	9 min	pseudo-first order	55
	solid PdCu nanoparticles	-	60min	pseudo-first order	55
	Pd black	-	70 min	pseudo-first order	55
	MnO_2 Nanorod	$NaBH_4$	unchanged	zero order	This work
	g-C_3N_4 Bulk	$NaBH_4$	15 min	zero order	This work
	Alg/CMC/Dex/Ca	$NaBH_4$	6 min	zero order	This work
	Alg/CMC/Dex/MnO_2/Ca	$NaBH_4$	5 min	pseudo-first order	This work
	Alg/CMC/Dex./MnO_2/g-C_3N_4/Ca	$NaBH_4$	1.20 min	pseudo-first order	This work
	Alg/CMC/Dex./MnO_2/g-C_3N_4/Ca	H_2SO_4	23.20 sec	pseudo-first order	This work

Determination of HOMO and LUMO energy states



UV-Vis absorption spectra of the nanocomposites of Alg/CMC/Dex/Ca, and Alg/CMC/Dex/MnO_2/Ca solutions are shown in Fig. The primary peak at 230 nm was assigned to π–π* transitions of aromatic C=C bonds in sp^2 hybridization region and peak at about 300 nm is attributed to the n–π* transition of C=O bonds (FT-IR). The plots between the square of the absorption energy (αhv, where α is the absorbance and hυ is the photon energy) against hv (Tauc plots), the direct band-gap energy values of Alg/CMC/Dex/Ca, Alg/CMC/Dex/MnO_2/Ca, Alg/CMC/Dex/MnO_2/g-C_3N_4/Ca are determined as 3.32 eV, 3.23 eV, 3.6eV respectively (inset in Fig. 2).

eduction peaks at −0.67,0.61, -1.34 V and an oxidationpeakat+0.50,+0.61,+0.81 V versus Ag/AgCl

It is clear that HUMO –LUMO gaps in all the composites are smaller in electrochemical study than Uv because electrochemical reuction of Cr(VI) to Cr(III) is faster than than Uv.

Fig. (a) UV-Vis absortion spectrum with Tauc plot of (a) Alg/CMC/Dex/Ca, (b) Alg/CMC/Dex/MnO_2/Ca, (c) Alg/CMC/Dex/MnO_2/g-C_3N_4/Ca, (d) Cyclic Voltammetry measurements of the Bare, Alg/CMC/Dex/Ca, Alg/CMC/Dex/MnO_2/Ca, Alg/CMC/Dex/MnO_2/g-C_3N_4/Ca, (e) HOMO and LUMO energy levels of nanocomposites determined by CV.

Cyclic voltammetry measurements determined the LUMO and HOMO energy levels of the Bare, Alg/CMC/Dex/Ca, Alg/CMC/Dex/MnO_2/Ca, Alg/CMC/Dex/MnO_2/g-C_3N_4/Ca to find the band-gap energy. Applying potentials above the LUMO to form an accumulation layer, or below the HOMO to form inversion layers, can lead to abrupt emergence of cathodic and anodic currents, respectively. Electrode for electrochemical analysis was prepared by nanocomposite suspensions (5 µl) with ethanol (0.5 µl) onto a glassy carbon electrode (diameter of 3 mm) and dried naturally at room temperature. Fig. 12(d) clears the performance of the GCE in the presence and absence of the as synthesized nanocomposites. The oxidation and reduction peaks related to electron and hole injections into the conduction and valence bands were consequently utilized to determine the E_{HOMO} and E_{LUMO} using the following three equations[56]

$$E_{HOMO} = -e\,(E_{Ox,vs.\ NHE} + 4.75)\ (eV)$$
$$E_{LUMO} = -e\,(E_{Red,vs.\ NHE} + 4.75)\ (eV)$$
$$E_{NHE} = E_{Ag/AgCl} + 0.197$$

The Alg/CMC/Dex/Ca, Alg/CMC/Dex/MnO_2/Ca, Alg/CMC/Dex/MnO_2/g-C_3N_4/Ca, showed reduction peaks at −0.67,0.61, -1.34 V and an oxidation peak at +0.50, +0.61, +0.81 V versus Ag/AgCl. The values of Alg/CMC/Dex/Ca, Alg/CMC/Dex/MnO_2/Ca, Alg/CMC/Dex/MnO_2/g-C_3N_4/Ca for E_{LUMO} and E_{HOMO} calculated from these peaks are E_{LUMO}= −4.3 eV,-4.19 eV, -3.99 eV and E_{HOMO}= −5.42, −5.48, −6.15 eV with increases to the x axis, respectively. The band-gap energy values calculated from the cyclic voltammetry graph for Alg/CMC/Dex/Ca, Alg/CMC/Dex/MnO_2/Ca, Alg/CMC/Dex/MnO_2/g-C_3N_4/Ca were 1.17, 1.22, 2.15 eV respectively.

X-Ray Photoelectron Spectroscopy

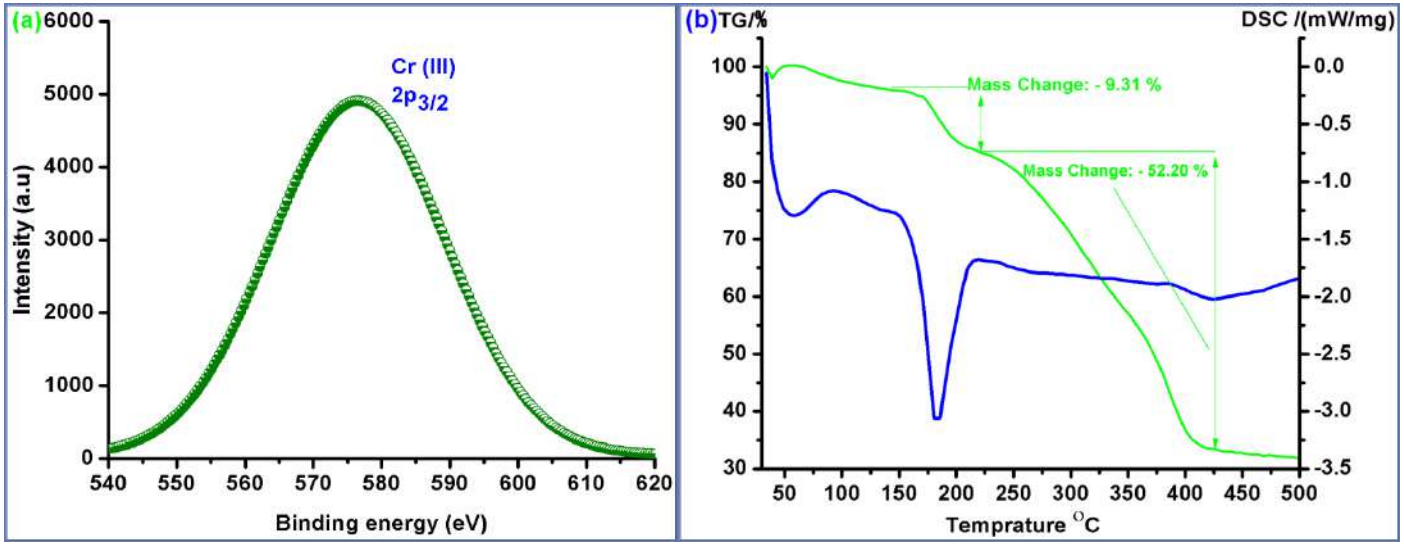


Fig.7(a) XPS studies of product Cr(III), (b) Thermogravimetric analysis (TGA) and differe thermogravimetric (DTG) curves of Alg/CMC/Dex/MnO_2/g-C_3N_4/Ca composite gels.

XPS spectra of Cr(III) as formed due to the reduction of Cr(VI) in presence of $NaBH_4$ revealed peak at 576.5 eV owing to 2p3/2 orbit under the present experimental conditions(Fig7 (a)).
TGA:From room temperature to 150ºC, slight mass of about 5% loss was observed as a result of removing of moisture followed by 9.31% loss of mass from 150ºC to 220ºC is attributed due to loss of excess dextran, alg. and CMC. Then 220ºC to 420ºC, a significant loss of mass 52.20% is observed due to the removal/decomposition of alginate, CMC, dextran. At end, about 33.5% Ca/MnO_2/g-C_3N_4 was left(Fig 7(b)). From the TGA/DTG results of the composite gels, it is concluded that composites are suitable for the catalytic applications owing to their efficient thermal stability.

Sheikh, M.U.D. and Pandit, U.J. and Naikoo, G.A. and Thomas, M. and Bano, M. and Ahirwar, D. and Khan, F.,Chemistry Select, Volume 2, Year 2017, Pages 9726-9735 (IF – 3.5

Gas chromatography–mass spectroscopic (GC–MS) study

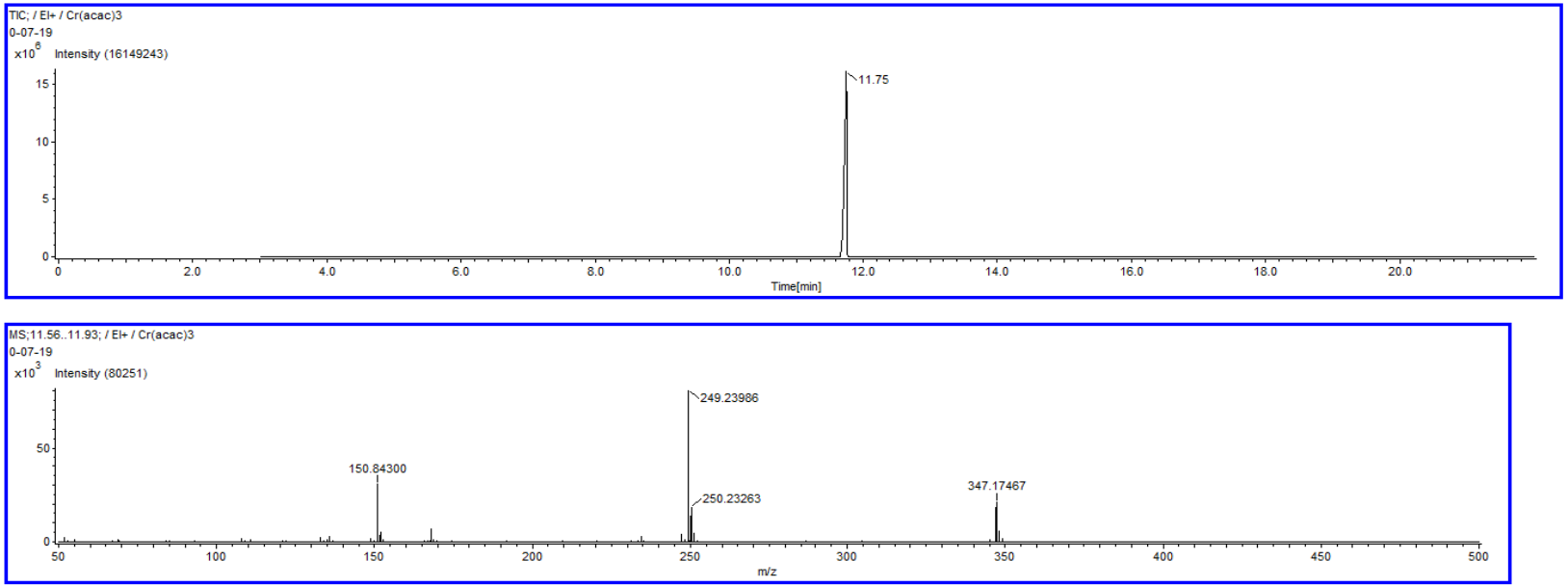


Fig. GC-MS

0.2 g $Cr(OH)_3$ and 0.1M HCl was taken in a beaker and heated at 200ºC in water bath, for 1 hour with constant stirring. The final product $CrCl_3$ thus obtained to get filtrated using filter paper. The product was in violet-green colour was dried in open air can be used for converting it to $Cr(acac)_3$ as procedure mentioned.[57]

GCMS analysis Fig. showed the GCMS graphs which clearly shows the retention time 11.75 min.

$$Cr(OH)_3 + 3HCl \rightarrow CrCl_3 + 3H_2O$$

The intensity against m/z plots attributed peaks at 150.84, 249.23 and 347.17

Thomas, M. and Naikoo, G.A. and Sheikh, M.U.D. and Bano, M. and Khan, F. Journal of Photochemistry and Photobiology A: Chemistry, **Volume** 327, **Year** 2016, **Pages** 33-43,
DOI:10.1016/j.jphotochem.2016.05.005

Thermodynamic Parameters

Energy of activation(Ea), and thermodynamic parameters such as enthalpy ($\Delta H^{\#}$) and entropy($\Delta S^{\#}$) were determined by Arrhenius's equation and Eyring equation[48] respectively. The value of Gibbs free energy ($\Delta G^{\#}$) was determined by the relation as

$$\Delta G^{\neq} = \Delta H^{\neq} - T\Delta S^{\neq} \quad (1)$$

The activation energy(E_a) for catalyst Alg/CMC/Dex/MnO_2/g-C_3N_4/Ca is 21.56 kJ mol^{-1}(Fig. S1) which confirms the reduction reaction is slow and surface controlled on catalyst surface. The value of enthalpy ($\Delta H^{\#}$) is 7.46 $kJmol^{-1}$(Fig.11) suggests that the reaction needs energy. The value of Gibbs free energy ($\Delta G^{\#}$) increases from 56.352 to 59.634 $kJmol^{-1}$ with increase of temperature confirmed that the reduction of Cr(VI) to Cr(III) required energy.The value of entropy($\Delta S^{\#}$) is -16.425$Jmol^{-1}K^{-1}$ at suggests that the reaction is feasible at higher temperature. [49] The temperature coefficient is 1.158 & 1.113 attributing the reaction is favorable at higher

Electrochemical Behaviours of different composites in presence of $K_2Cr_2O_7$ Solution

A: (a) Alg/CMC/Dex/MnO_2/g-C_3N_4/Ca-CPE, (b) Alg/CMC/Dex/MnO_2/Ca-CPE, © Alg/CMC/Dex/Ca-CPE, (d) bare-CPE

Thomas, M. and Naikoo, G.A. and Sheikh, M.U.D. and Bano, M. and Khan, F. Reactive and Functional Polymers, Volume 105, Year 2016, Pages 78-88(IF 3.6)

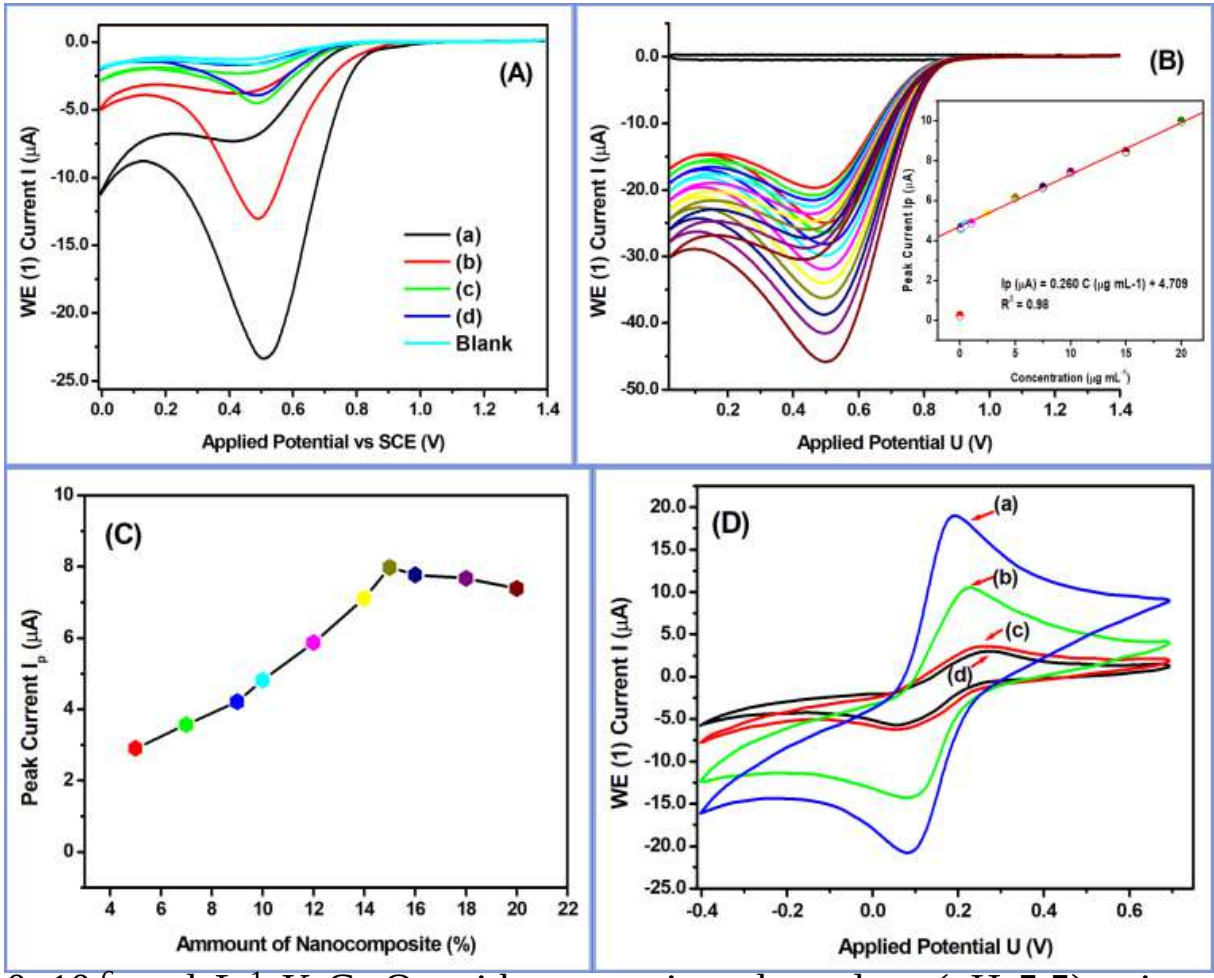
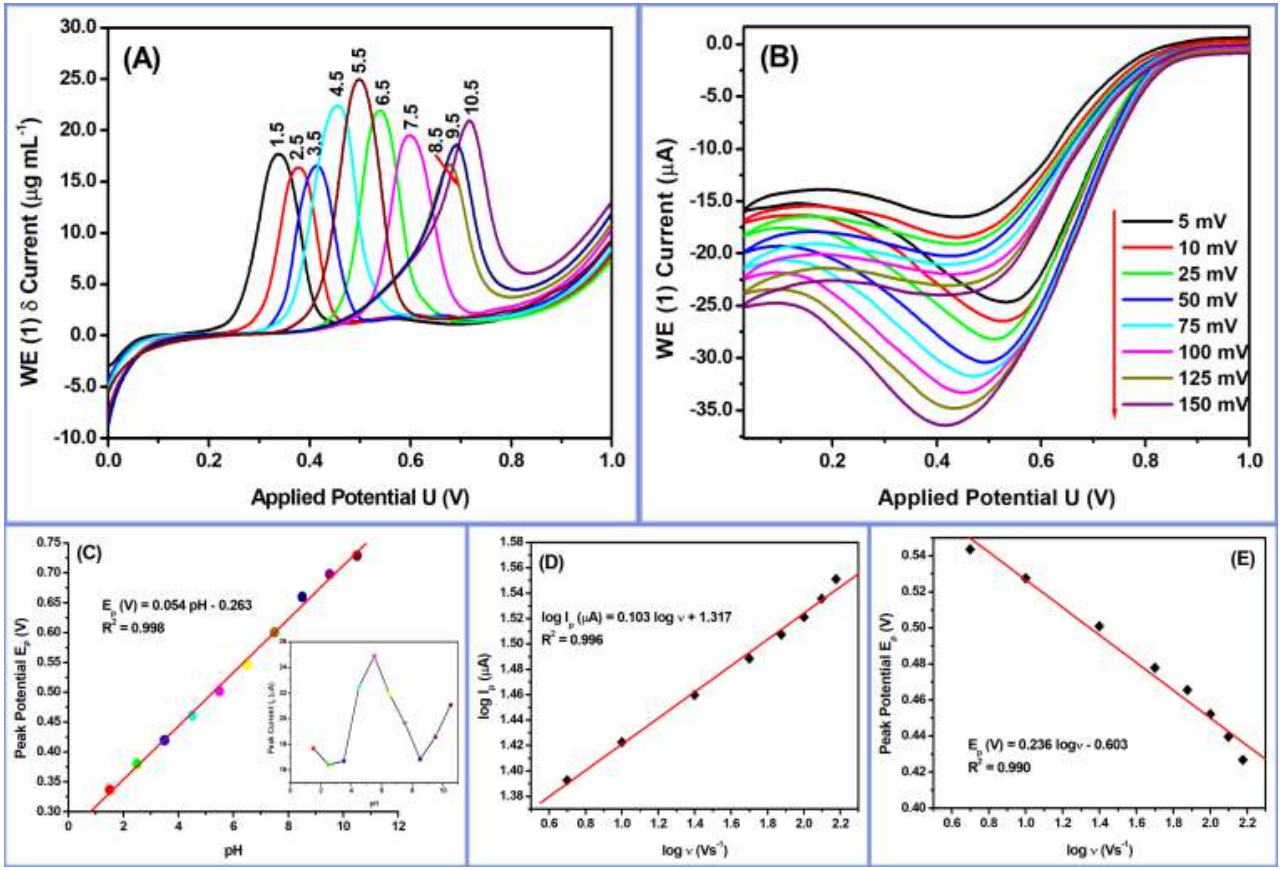


Fig 8: Cyclic voltammogram of (A) 1.0×10^{-6} mol L^{-1} $K_2Cr_2O_7$ with supporting electrolyte (pH 5.5) using modified composites-CPE (B) Cyclic voltammogram of variable concentration of $K_2Cr_2O_7$ ranges from **0.01 to 20.0 µM** at Alg/CMC/Dex/MnO_2/g-C_3N_4/Ca-CPE; Blank voltammogram in (A) and (B) shows the redox activity of Alg/CMC/Dex/MnO_2/g-C_3N_4/Ca-CPE without $K_2Cr_2O_7$ in acetate buffer (pH 5.5); (C) Influence of amount of Alg/CMC/Dex/MnO_2/g-C_3N_4/Ca in total paste material on DPV determination of Cr (VI) ion, (D) Cyclic voltammogram of 1.0 mM $Fe(CN)_6^{3-/4-}$ in 0.1 M KCl at (a) Alg/CMC/Dex/MnO_2/g-C_3N_4/Ca-CPE, (b) Alg/CMC/Dex/MnO_2/Ca-CPE, (c) Alg/CMC/Dex/Ca-CPE and (d) bare-CPE.

1.Electrode optimization

In the fabrication of electrode, the composition of graphite powder, nanocomposite with pasting liquid (paraffin oil) strongly affects the reactivity of electrode. The increase in the amount of pasting liquid decreases electron transfer rates as well as the background current contributions.[37-38] The optimum amount of Alg/CMC/Dex/MnO_2/g-C_3N_4/Ca nanocomposite mixed with graphite powder to fabricate Alg/CMC/Dex/MnO_2/g-C_3N_4/Ca/CPE was achieved by varying the amount of Alg/CMC/Dex/MnO_2/g-C_3N_4/Ca from 5% to 20% (w/w) in total paste material and their peak response were analysed by recording differential pulse voltammogram (DPV) of 1.0×10^{-6} $molL^{-1}$ $K_2Cr_2O_7$ in acetate buffer pH 5.5 (Figure 7C). The best electrode response was obtained with 15% (w/w) of nanocomposite 60% (w/w) graphite powder and 25% (w/w) paraffin oil. Similarly in case of Alg/CMC/Dex/Ca/CPE and Alg/CMC/Dex/MnO_2/Ca/CPE, 15% (w/w) of Alg/CMC/Dex/Ca and Alg/CMC/Dex/MnO_2/Ca in total paste material shows the best peak response for 1.0×10^{-6} mol L^{-1} $K_2Cr_2O_7$.

Evaluation of electrode-analyte kinetic parameters



Optimum pH is 5.5

Fig 9: **(A)** DPV of 1×10^{-6} M $K_2Cr_2O_7$ in different pH values, **(B)** Cyclic Voltammograms of $K_2Cr_2O_7$ at different scan rates ranging from 5-150 mVs^{-1} using Alg/CMC/Dex/MnO_2/g-C_3N_4/Ca-CPE; **(C)** Variation of peak potential and peak current (Inset graph) of 1×10^{-6} M $K_2Cr_2O_7$ with pH; **(D)** and **(E)** Effect of scan rate showing Plot of E_p vs log ν and Plot of log I_p vs log ν.

Ahirwar, D. and Bano, M. and Khan, F., Journal of Sol-Gel Science and Technology, Volume 79, Year 2016, Pages 228-237, If – 2.0

To probe the electroactive surface area of all fabricated CPEs, cyclic voltammograms of 1.0 mM $K_3Fe(CN)_6$ probe in 0.1 M KCl were recorded with variable scan rate. The reversible one electron redox behavior of $Fe(CN)_6^{3-/4-}$ ions were obtained. By applying the Randles-Sevick equation[39] and the slope value of plot of I_{pa} versus $\upsilon^{1/2}$, the surface area for b-CPE, Alg/CMC/Dex/Ca-CPE, Alg/CMC/Dex/MnO_2/Ca-CPE and Alg/CMC/Dex/MnO_2/g-C_3N_4/Ca-CPE was calculated as 0.035 cm^2, 0.280 cm^2, 0.816 cm^2 and 1.155 cm^2 respectively.

$$I_{pa} = 0.4463 \left(\frac{F^3}{RT}\right)^{1/2} n^{3/2} A_0 D_0^{1/2} C v^{1/2} \qquad \text{-----1}$$

Where, I_{pa} is Anodic peak current, A_0 is electroactive surface area of electrode (cm^2), R is molar gas constant (8.314 $JK^{-1}mol^{-1}$), and F is Faraday's constant (96540 C mol^{-1}), D_0 is diffusion coefficient (1.0 mM concentration C of $Fe(CN)_6^{3-/4-}$), and T is Kelvin temperature. However, the ΔE_p (anodic and cathodic peak separation) values of b-CPE, Alg/CMC/Dex/Ca-CPE, Alg/CMC/Dex/MnO_2/Ca-CPE and Alg/CMC/Dex/MnO_2/g-C_3N_4/Ca-CPE were evaluated from cyclic voltammograms of scan rate, 50 mVs^{-1} as 0.295 V, 0.213 V, 0.155 V and 0.101 V respectively (**Fig 8D**). **The gradual decreases in ΔE_p and increase in peak current value upon subsequent modification of electrode surface indicate the increase in conductivity of electrode and favors easier and faster charge transfer**.

The pH medium and the supporting electrolyte contribute a substantial impact on electrochemical response of analyte and their evaluation of redox mechanism. The electrocatalytic reduction reaction of $K_2Cr_2O_7$ was analyzed in different buffer mediums *i.e.* Acetate, phosphate, citrate and Britton-Robinson buffer solution in variable pH range using DPV. The best voltammetric response in terms of current intensity was obtained with 0.02 M acetate buffer (**Fig 9A**). A linear relationship is obtained in the plot of peak potential (E_P) *vs* solution pH (**Fig 9C**) shows slope value is 54 $mVpH^{-1}$, close to Nernstian theoretical value of 59 $mVpH^{-1}$. It indicates the equal number of electrons and protons involved in electrode reduction process. The plot of peak current (I_p) *vs* pH (**Fig 9C inset**) depicted that peak current was obtained highest at pH 5.5, thus reduction rate was high at pH 5.5, considered as favorable pH value for subsequent electrostatic interaction between catalytic nanocomposite functionalities and analyte.

The cyclic voltammetric study of 1×10^{-6} M $K_2Cr_2O_7$ (pH 5.5) with variable scan rate [1] (5-150 mVs^{-1}) using Alg/CMC/Dex/MnO_2/g-C_3N_4/Ca-CPE reveals various electrode kinetic parameters and the nature of electrode reaction. **The superposed voltammograms revealed that the augment in scan rate value consequently increase of peak current (I_p) and shift of peak potential (E_p) towards negative potential, confirms the irreversible nature of reduction process** (**Fig 9B**). The plot of log I_p *vs* log υ shows a linear relationship (**Fig 9D**), expressing the equation: log I_p (μA) = 0.104 log υ + 1.317; R^2 = 0.996. The obtained slope value, 0.1 was close to proximity of theoretical Nernstian value of 0.1 for typical adsorption controlled electrode reaction [40]. The plot of E_p *vs* log υ (**Fig 8E**) also exhibit linearity with correlation coefficient of 0.990, again confirms the irreversible and adsorptive controlled electrode process. For irreversible electrode reaction Laviron's equation [41] is expressed as:

mV

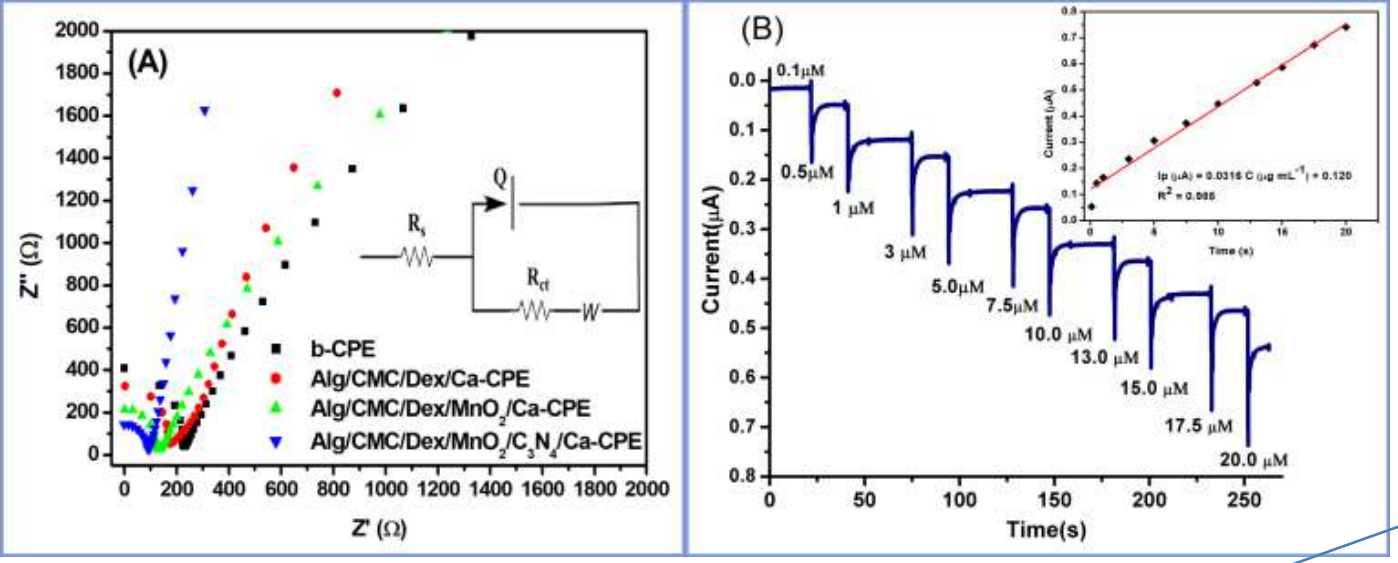
$$W_{1/2} = \frac{2.44RT}{\alpha nF} = \frac{0.0626}{\alpha n} \quad \text{----- 2}$$

$$E_p = E^0 + \left(\frac{2.303RT}{\alpha nF}\right) log \frac{RTK^0}{\alpha nF} + \left(\frac{2.303RT}{\alpha nF}\right) log\, v \quad \text{--- 3}$$

$$\alpha = \frac{47.7}{E_p - E_{p/2}} \quad \text{----- 4}$$

Where, υ represents scan rate and $W_{1/2}$ is half width of peak. The slope value of E_p *vs* log υ gives the value of αn, calculated to be 0.2365 and by putting the values of R, F and T = 298 K in equation 2, αn was calculated to be 0.2504. The fractional αn values further confirms the existence of irreversible reduction reaction. According to Bard and Faulkner's equation [42] .

Where, E_p is peak potential, $E_{P/2}$ is half peak potential where current is at half of the peak value. The value of electron transfer coefficient (α) was amounted to be 0.0805 and the number of electron transferred (n) was amounted to be 3. The value of formal redox potential (E^o) was calculated by extrapolating the plot E_p *vs* log υ to vertical axis at υ = 0 and from the intercept, E^o was amounted to be 0.603. Thus from equation 3, the value of standard heterogeneous rate constant (k^o) was calculated as 2.138×10^2 cm s^{-1}. The degree of surface coverage (Γ^*) of all nanocomposite modified and bare CPEs for electroreduction of 1×10^{-6} M $K_2Cr_2O_7$ is determined by using following relationship:[39, 43]



$$k_{app} = \frac{RT}{F^2 R_{ct} C} \quad \text{---- 6}$$

Fig.10 (A) Nyquist plots for all nanocomposite modified CPEs at an amplitude of 10.0 mV Vs Ag/AgCl over the frequency range of 0.1 Hz to 10^6 Hz in 1.0 mM $K_2Cr_2O_7$ in 0.1 M KCl; **(B)** Amperometric sensing performance of variable concentration of $K_2Cr_2O_7$ varied from 0.01μM to 20 μM at Alg/CMC/Dex/MnO_2/g-C_3N_4/Ca-CPE, inset graph shows calibration curve exhibiting a linear response of peak current with $K_2Cr_2O_7$ concentration.

Where C is the concentration of $K_2Cr_2O_7$ and other terms have their usual meaning. The k_{app} values are presented in **Table 2** confirms the excellent electrocatalytic property of Alg/CMC/Dex/MnO_2/g-C_3N_4/Ca-CPE in addition to faster electron transfer rate, high aspect ratio and good conductivity. In **Fig 9A inset** shows the electrical equivalent circuits compatible with impedance spectra where R_s represents solution resistance, Q is double-layer capacitance and W is finite-length Warburg short-circuit term coupled to R_{ct}. **(Z' represents real part of impedence and Z'' imaginary part of impedance).**

Dar, R.A. and Naikoo, G.A. and Kalambate, P.K. and Giri, L. and Khan, F. and Karna, S.P. and Srivastava, A.K.,Electrochimica Acta, Volume 163, Year 2015, Pages 196-203, (Impact Factor 6.6)

$$I_{pa} = (n^2F^2/4RT)\,\Gamma^* Av \quad \text{---- 5}$$

Where I_{pa} represents Anodic peak potential of cyclic voltammogram, 'A' electrode surface area, 'v' scan rate and other terms have their usual meanings. The results tabulate in **Table 2**, evident that Alg/CMC/Dex/MnO_2/g-C_3N_4/Ca-CPE displays maximum surface coverage (**Γ^*) values** towards determination of Cr(VI). The Nyquist plot of 1×10^{-6} mol L^{-1} $K_2Cr_2O_7$ in acetate buffer pH 5.5 and 0.01 M KCl on all nanocomposite modified and bare CPEs (**Fig 9A**) was studied via electrochemical impedance spectroscopy (EIS) probe the ultra-capacitor properties, charge transfer properties and double layer capacitance of electrode interfac.[38] The semicircle element experiential at high frequency region (10^{-1}-10^6 Hz) reveals the charge transfer limiting process. The diameter of semicircle probes the charge transfer resistance (R_{ct}).[44] The Alg/CMC/Dex/MnO_2/g-C_3N_4/Ca-CPE shows lowest R_{ct} value (85 Ω) than other modified and bare CPEs, depicted in **Table 2**. The incorporation of g-C_3N_4 and MnO_2 in nanocomposite material increases the conductivity and their addition in graphite paste make the surface more conductive. The result expresses a considerable difference in electrochemical performance and conductivity of all designed electrodes. The subsequent modification of electrode surface consequences the gradual decrease in diameter of semicircle domains and thus R_{ct} values, furthermore it confirms the successful electro-reduction of Cr at electrode surface. The value of apparent electron-transfer rate constant (k_{app}) was calculated by using equation (5):[38,39]

Table 2: R_{ct}, k_{app}, and Γ^* values of all modified electrodes.

Electrode	R_{ct} (Ω)	k_{app} (10^{-6} cm s^{-1})	Γ^* (10^{-12} mol cm^{-2})
b-CPE	405	6.572×10^{-7}	2.622
Alg/CMC/Dex/Ca-CPE	245	1.086×10^{-6}	3.907
Alg/CMC/Dex/MnO_2/Ca-CPE	165	1.613×10^{-6}	38.414
Alg/CMC/Dex/MnO_2/g-C_3N_4/Ca-CPE	85	3.131×10^{-6}	48.502

Γ^* = surface coverage

In Nyquist **plot Z' represents real part of impedence and Z'' imaginary part of impedance.** On the left side (High frequency side) a semicircle which is followed by straight line (as you proceed right) indicates capacitive behaviour. ESR and various charge transfer resistence including Wirburg parameters are obtained from EIS.

Analytical determination

The quantification capability and sensitivity of sensor towards Cr ions was demonstrated by recording the amperometric curves (**Fig 10B)** of different concentration of $K_2Cr_2O_7$ in 0.02 $molL^{-1}$ acetate buffer (pH 5.5 ± 0.01) and 0.01 M KCl solution using Alg/CMC/Dex/MnO_2/g-C_3N_4/Ca-CPE at 0.3V. The designed electrode exhibited a rapid response to the addition of $K_2Cr_2O_7$ followed by a steady–state within 1.2 s. **Figure 10B inset** exhibited a linear relationship between the reduction peak current and $K_2Cr_2O_7$ concentration in the range of 0.01 - 20.0 µg $mL^{-1}$with linear regression equation as: Ip (µA) = 0.0316 C (µg mL^{-1}) + 0.120 with a correlation coefficient of 0.985. The limit of detection and the limit of quantification were calculated to be 0.00063 µg mL^{-1} (0.63 ng mL^{-1}) and 0.00210 µg mL^{-1} respectively. The sensitivity was amounted to be 0.303 µA mM^{-1} cm^{-2}. The comparative account of analytical characteristics of designed electrode for determination of Cr with some other reported methods is represented in **Table S1**.

$$\mathbf{LOD = 3s/m} \qquad \text{----1}$$

$$\mathbf{LOQ= 10s/m} \qquad \text{-----2}$$

where, s is the standared deviation of the intercept, and m is the slope of the regression line.

Conclusion

We have successfully reduced Toxic Cr(VI) to Cr(III) using Alg/CMC/Dex/MnO_2/g-C_3N_4/Ca composites in presence of NaBH4 in 1.20 min. The as synthesized monolith (Alg/CMC/Dex/MnO_2/g-C_3N_4/Ca/CPE is also used as sensor to detect Cr(VI) upto a level of 0.63 ng mL^{-1} . The activation energy(Ea) for catalyst Alg/CMC/Dex/MnO2/g-C3N4/Ca is 21.56 kJ mol-1(Fig. S1) which confirms the reduction reaction is slow and surface controlled on catalyst surface. Thermodynamic parameters such as ΔG, ΔH and Δ S also confirmed that the reaction is favorable at higher temperature.

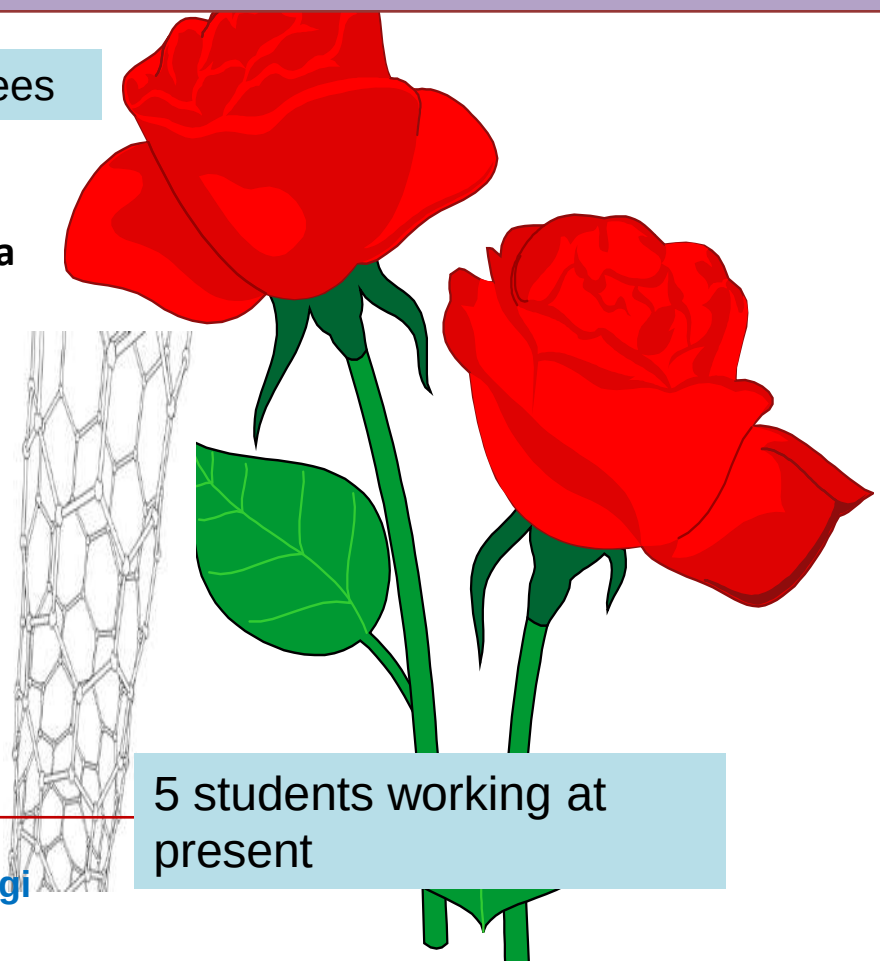
The whole process is non –toxic, economically viable and environmentally benign.

THANKS

1.DST, Project (Nanomission), Govt. of India, (2014-2018) funded amount Rs. 1,57,53,000 = 00 (One Crore, fifty seven lakhs & fifty three thousands).

Conferred Ph.D degrees

1. **Miss Krishna Nema**
2. **Miss Ratna Dodke**
3. **Firoj Khan**
4. **Alok Jain**
5. **Ilyas Ansari**
6. **Seema Vajhallya**
7. **Ahshan Zaidi**
8. **Laxmi Tantuyoy**
9. **Amul Kumar**
10. **Miss Afroja Khanam**
11. **Puran Lal Sahu**
12. **S. N. Chadar**
13. **Malkhan S Parihar**
14. **Miss Rakhi Agarwal**
15. **Miss Ruchi Bilgainya**
16. **Miss Kavita Rai**
17. **G. A. Naikoo**
18. ***Molly Thomas***
19. **M. U-din Sheikh**
20. **Devendra Ahirwar**
21. **Mustari Bano**
22. **Mansi Rai**
23. **Ankita Nema**
24. **Sambhoyna S Dangi**
25. **Kabya Srivastava**



5 students working at present